20 May 1999

Membrane Process for Biological Treatment of Contaminated Gas Streams

Sarina J. Ergas

Leslee Shumway

Mark W. Fitch
Missouri University of Science and Technology, mfitch@mst.edu

Jeffrey J. Neemann

Recommended Citation

S. J. Ergas et al., "Membrane Process for Biological Treatment of Contaminated Gas Streams," *Biotechnology and Bioengineering*, vol. 63, no. 4, pp. 431 - 441, Wiley, May 1999.
The definitive version is available at https://doi.org/10.1002/(SICI)1097-0290(19990520)63:4<431::AID-BIT6>3.0.CO;2-G

eppendorf

Boost Your (Stem) Cell Culture

We assist you to scale up your bioprocess –
Eppendorf Bioprocess Solutions for Cell & Gene Therapy Development - Flexibe, Scalable, Industrial

The BioFlo® 320 offers flexibility, better control, and maximum functionality while occupying a fraction of the valuable lab space of similar systems. This means greater efficiency and productivity at a lower operating cost for your lab. BioBLU® Single-Use Bioreactors were developed as true replacements for existing reusable vessels.

- > Sterility Assurance Level (SAL): 10^{-6}
- > Simplified handling reduces cross-contamination
- > Reliable scalability from 250 mL - 40 L through industrial design
- > Proven for animal and human cell lines
- > Increased productivity with reduced turnaround time between runs

www.eppendorf.com/BioBLUc

Membrane Process for Biological Treatment of Contaminated Gas Streams

Sarina J. Ergas,[1] Leslee Shumway,[2] Mark W. Fitch,[3] Jeffrey J. Neemann[4]

[1]Department of Civil and Environmental Engineering, University of Massachusetts, Amherst, Massachusetts 01003; telephone: (413) 545-3424; fax: (413) 545-2202; e-mail: ergas@ecs.unmass.edu
[2]Space and Naval Warfare Systems Center, San Diego California
[3]Department of Civil Engineering, University of Missouri—Rolla, Rolla, Missouri
[4]Black & Veatch, 8400 Ward Parkway, Kansas City, Missouri 64114

Received 1 June 1998; accepted 8 November 1998

Abstract: A hollow fiber membrane bioreactor was investigated for control of air emissions of biodegradable volatile organic compounds (VOCs). In the membrane bioreactor, gases containing VOCs pass through the lumen of microporous hydrophobic hollow fiber membranes. Soluble compounds diffuse through the membrane pores and partition into a VOC degrading biofilm. The hollow fiber membranes serve as a support for the microbial population and provide a large surface area for VOC and oxygen mass transfer. Experiments were performed to investigate the effects of toluene loading rate, gas residence time, and liquid phase turbulence on toluene removal in a laboratory-scale membrane bioreactor. Initial acclimation of the microbial culture to toluene occurred over a period of nine days, after which a 70% removal efficiency was achieved at an inlet toluene concentration of 200 ppm and a gas residence time of 1.8 s (elimination capacity of 20 g m^{-3} min^{-1}). At higher toluene loading rates, a maximum elimination capacity of 42 g m^{-3} min^{-1} was observed. In the absence of a biofilm (abiotic operation), mass transfer rates were found to increase with increasing liquid recirculation rates. Abiotic mass transfer coefficients could be estimated using a correlation of dimensionless parameters developed for heat transfer. Liquid phase recirculation rate had no effect on toluene removal when the biofilm was present, however. Three models of the reactor were created: a numeric model, a first-order flat sheet model, and a zero-order flat sheet model. Only the numeric model fit the data well, although removal predicted as a function of gas residence time disagreed slightly with that observed. A modification in the model to account for membrane phase resistance resulted in an underprediction of removal. Sensitivity analysis of the numeric model indicated that removal was a strong function of the liquid phase biomass density and biofilm diffusion coefficient, with diffusion rates below 10^{-9} m^2 s^{-1} resulting in decreased removal rates. *Biotechnol Bioeng* **63:** 431–441, 1999.
Keywords: volatile organic compounds; hollow fiber membranes; biological treatment; air pollution control; modeling

Correspondence to: S. J. Ergas
Contract grant sponsor: National Science Foundation
Contract grant number: BES-9530592

INTRODUCTION

Biofiltration is a low cost and effective method for controlling air emissions of biodegradable volatile organic compounds (VOCs). Studies and field applications of these systems, however, have been limited to inlet VOC loading rates of less than 50 g m^{-3} h^{-1}. At high VOC loading rates, microbial growth results in clogging of media pore spaces. In addition, these systems are of limited use where degradation results in the formation of acidic metabolites (e.g., methylene chloride), where co-substrates must be added to induce enzymes required for cometabolism (e.g. trichloroethene), or where anaerobic conditions must be maintained in the system (e.g. tetrachloroethene).

A hollow fiber membrane bioreactor (HFMB) is currently under investigation that has the potential to overcome the limitations described above. The HFMB utilizes hydrophobic microporous hollow fiber membranes that serve as a support for the microbial population and provide a large surface area for VOC and oxygen mass transfer. Waste gases containing VOCs are passed through the lumen of the hollow fiber membranes. Soluble compounds in the gas phase are transferred through the membrane pores and partition into a VOC degrading biofilm surrounded by a circulating nutrient media. Compounds in the biofilm are available for biodegradation. The reactor is also designed to provide a method for wasting biomass to prevent clogging at high VOC loading rates. In addition, pH buffers, nutrients, and/or co-substrates may be added to the system to support the microbial population and neutralize acidic metabolites.

Hollow fiber membranes have been used previously in a number of gas transfer applications including: air stripping of VOCs from contaminated water (Castro and Zander, 1995; Semmens et al., 1989), recovery of cyanide from wastewater (Shen et al., 1997), bubble-free aeration of bioreactors (Ahmed and Semmens, 1992, 1996; Coté et al., 1988, 1989), and biological treatment of VOCs in wastewaters (Aziz et al., 1996; Freitas dos Santos and Livingston, 1995a; Pavasant et al., 1996). Several authors have also investigated the use of HFMBs for treatment of gas phase

 CCC 0006-3592/99/040431-11

VOCs (Ergas and McGrath, 1997; Hartmans et al., 1992; Parvatiyar et al., 1996a,b; Reij et al., 1995, 1997).

Hartmans et al. (1992) first reported using a HFMB for the control air emissions of toluene and dichloromethane. A number of different membrane materials were tested. Their experiments resulted in greater than 95% removal of toluene and dichloromethane.

A flat sheet microporous polypropylene HFMB was used by Reij et al. (1995) to remove propene from a gas stream. After five days with an inlet propene concentration of 2300 ppm, the biofilm acclimated and 58% propene removal was maintained for the duration of the thirty-day test. Because propene is a poorly soluble compound, all mass transfer resistance was found to be in the liquid phase. For more soluble compounds, the authors determined that membrane phase resistance could approach the same order of magnitude as liquid phase resistance.

Parvatiyar et al. (1996a) used a two module-in-series polysulfone HFMB to investigate toluene removal from a contaminated airstream. Toluene removal reached 84% with a 16-second gas residence time and an inlet concentration of 600 ppm_v. A similar experimental system was used by the authors to study degradation of trichloroethylene (TCE) (Parvatiyar et al., 1996b). The biofilm was initially acclimated to toluene and then gradually weaned from a toluene/TCE mixture to 100% TCE. A 30% TCE removal efficiency was achieved with a 36-s gas residence time.

In a previous study (Ergas and McGrath, 1997) a polyethylene HFMB was used for removal of toluene from a contaminated airstream. Removal efficiencies of greater than 97% were achieved with an inlet toluene concentration of 100 ppm_v and a gas residence time of 1.4 s. Removal efficiency was found to decrease over time, however, due to clogging of the bioreactor with microbial biomass. Mathematical modeling assumed that mass transfer resistance was dependent on liquid phase resistance and that gas and membrane resistances were negligible. Abiotic reactor testing demonstrated that, with no biofilm present, mass transfer was dependent on liquid phase turbulence.

The objective of this research was to further investigate the use of a HFMB for removal of toluene from a gas stream and to determine the effects of varying operating conditions on reactor performance. Toluene was used as a model compound in these experiments because its biodegradation is well understood. Specific objectives included (1) determination of the effect of liquid phase turbulence on toluene mass transfer in an abiotic (no biofilm) HFMB, (2) determination of the effects of toluene loading rate, gas residence time, and liquid phase turbulence on toluene removal efficiency in a laboratory-scale membrane bioreactor, (3) determination of the effect of nitrogen source (NH_4^+ or NO_3^-) on toluene biodegradation rate and biomass yield, and (4) refinement and testing of mathematical models of mass transfer and biodegradation.

THEORETICAL DEVELOPMENT

The continuity equation incorporating Monod kinetics cannot be solved analytically for a biofilm, therefore a large number of biofilm models have been developed. Most often, either simplifying assumptions are made or a complex set of nonlinear equations is solved numerically (Saez and Rittmann, 1988). Recent research has shown that biofilms are much more complex than as described by simple biofilm models. Transport of dissolved compounds is not solely due to diffusion. Transport of particulate matter is not solely due to microbial growth. In addition, biofilms have been shown to have nonconstant porosity and continuous attachment and detachment of cells (Wanner, 1995). Nonetheless, relatively simple models of substrate diffusion and reaction have been validated using microsensor measurements (Cunningham et al., 1995).

Simple first- and zero-order approximation models of biofilm diffusion and reaction may be found in most bioengineering texts. In most cases, however, first- and zero-order approximations do not reflect the substrate concentration actually found in a biofilm (Saez and Rittmann, 1990). Saez and Rittmann (1988) developed a pseudoanalytical solution for substrate flux in a biofilm at steady state that was accurate over a wide range of substrate concentrations. A similar approach resulted in an algebraic solution that was accurate for a fully penetrated biofilm (Kim and Suidan, 1989). Studies using toluene in a flat plate vapor phase reactor resulted in a complex model incorporating growth, inhibition, and decay kinetics which fit observed concentrations in the reactor with adjustment of the parameters for biofilm density, endogenous decay rates, and death rates (Mirpuri et al., 1997; Villaverde et al., 1997).

The system reported here differs from all of the models described above in that the general biofilm model uses an inert surface to establish a boundary condition, with substrate entering the biofilm from the liquid interface. In a membrane biofilter, substrate partitions from the gas phase to the membrane surface, enters from the solid support side, diffuses through and is degraded in the biofilm, diffuses across the liquid interface, and is then degraded in the liquid phase. A conceptual model of this system is shown in Fig. 1.

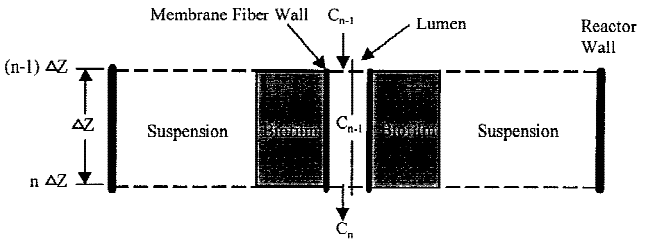

Figure 1. Conceptual model of the phases of the hollow fiber membrane reactor.

Abiotic Mass Transfer Model

An analytical solution was developed for mass transfer in an abiotic hollow fiber membrane reactor. The abiotic mass transfer model was used to evaluate the overall mass transfer coefficients from the experimental data.

In the absence of a biofilm, the VOCs diffuse through the membrane pores, then through a stagnant liquid film, then to the bulk liquid phase which is treated as a continuous-flow stirred-tank reactor (CFSTR). The liquid phase concentration may be kept low by flushing liquid from the reactor, much like the operation of a scrubber. The concentrations at the interface between the membrane and liquid phases can be described by Henry's law:

$$S_L = C_g/H, \tag{1}$$

where H is the Henry's law coefficient, C_g is the gas phase concentration, and S_L is the liquid phase concentration. The flux from the gas phase to the liquid phase, J, can be described by

$$J = KA(C_g - HS_L), \tag{2}$$

where K is the overall mass transfer coefficient and A is the membrane surface area. A series resistance model may be used to describe K:

$$\frac{1}{K} = \frac{1}{k_g} + \frac{1}{k_m} + \frac{H}{k_l}, \tag{3}$$

where k_g, k_l, and k_m are the local mass transfer coefficients in the gas, liquid, and membrane phases, respectively. Previous authors (Yang and Cussler, 1986; Semmens et al., 1989; Ergas and McGrath, 1997) have used correlations of dimensionless parameters to estimate mass transfer coefficients for hollow fiber air strippers and bubbleless aeration systems. Knudsen and Katz (1958) developed the following equation to estimate heat transfer coefficients for fluid flowing in ducts:

$$\mathrm{Sh} = 45.45\mathrm{Re}^{0.6}\,\mathrm{Sc}^{0.33}, \tag{4}$$

where Sh is the Sherwood number (Kd/D_s), Re is the Reynolds number ($d_e v_L/\nu$), and Sc is the Schmitt number (ν/D_s). The effective diameter, d_e, is calculated as four times the area over the wetted perimeter. At steady state, the transport equation for VOCs in the gas phase is

$$v_z \frac{dC_g}{dz} = Ka(C_g - HS_L), \tag{5}$$

where v_z is the gas velocity in the fibers and a is the membrane surface area per unit volume. With the boundary condition $C_g = C_o$ (the inlet concentration) at $z = 0$, Eq. (5) integrates to

$$\ln\left[\frac{C_g - HS_l}{C_o - HS_L}\right] = \frac{-KaL}{v_z}, \tag{6}$$

where L is the length of the fibers.

Biofilm Model

A model was derived for a single lumen and related to the total removal by the number of lumen. Model assumptions included: steady state operation; Monod biodegradation kinetics; and constant biomass density, ρ_b. Because concentration varies both axially and radially, no analytical solution exists for a single lumen. Therefore, the lumen is divided along the axis into n sections, each with an axial length, Δz. The influent gas concentration to the nth section (see Fig. 1) is the concentration exiting the previous section, C_{n-1}. The concentration exiting the nth section, C_n, is equal to the influent less the removal in the section due to the mass transfer and biodegradation.

Membrane Mass Transfer

The flux, J_n, of substrate through the membrane can be expressed as

$$J_n = k_m A_m (C_{n,m} - C_{n-1}), \tag{7}$$

where k_m is the membrane mass transfer coefficient, A_m is the area of the membrane in the section, and $C_{n,m}$ is the gas phase concentration on the outer face of the membrane. A number of authors have assumed that gas and membrane resistances are negligible compared to liquid phase resistance (Ergas and McGrath, 1997; Yang and Cussler, 1986; Coté et al., 1989) and therefore $C_{n,m}$ is approximately equal to the concentration in the gas stream, C_{n-1}. Since the membrane is surrounded by biofilm, the liquid phase concentration at the biofilm interface, $S_{n,0}$, can be related to $C_{n,m}$ ($= C_{n-1}$) by Henry's constant:

$$S_{n,0} = C_{n-1}/H. \tag{8}$$

Eq. (8) sets the inner surface (left-hand) boundary condition for the biofilm model.

Suspension Mass Transfer and Degradation

The suspension (liquid volume) is treated as a CFSTR. The mass flux of the substrate, J_b, from the biofilm to the liquid can be described by

$$J_b = k_L A_B (S_{n,i} - S_L) \tag{9}$$

where k_L is the liquid mass transfer coefficient, A_b is the outer surface area of the biofilm, $S_{n,i}$ is the VOC concentration at the outer surface of the biofilm, and S_L is the bulk liquid VOC concentration. If we assume Monod biodegradation kinetics, a mass balance on the liquid volume yields

$$\frac{\rho_L}{Y}\frac{\mu_{max} S_L}{K_S + S_L} V = QS_o - QS_L + J_b, \tag{10}$$

where V is the liquid volume, ρ_L is the biomass density in the liquid, μ_{mass} is the maximum specific growth rate, Y is the yield coefficient, K_S is the half–saturation coefficient, Q

is the liquid flow rate, and S_o is the influent VOC concentration to the suspension.

Substituting Eq. (9) into (10) and solving for $S_{n,i}$ yields

$$S_{n,i} = \left(1 + \frac{V\rho_L\mu_{max}}{Yk_LA_b\,(K_S + S_L)}\right)S - \frac{Q}{k_LA_b}\,(S_o - S_L) \qquad (11)$$

This relationship sets the exterior surface (right-hand) boundary condition for the biofilm model.

Biofilm Mass Transfer and Degradation

The continuity equation in cylindrical coordinates (r, z, and θ) for the biofilm is

$$\frac{\partial S}{\partial t} + \left(v_r\frac{\partial S}{\partial r} + v_\theta\frac{1}{r}\frac{\partial S}{\partial \theta} + v_z\frac{\partial S}{\partial z}\right) = D_S\left(\frac{1}{r}\frac{\partial}{\partial r}\left(r\frac{\partial S}{\partial r}\right) + \frac{1}{r^2}\frac{\partial^2 S}{\partial \theta^2} + \frac{\partial^2 S}{\partial z^2}\right) + R_s, \qquad (12)$$

where S is the substrate concentration in the biofilm, D_S is the VOC diffusion coefficient in the biofilm, v_r, v_θ, v_z are the velocities in the r, θ, and z directions, respectively, and R_s is the substrate utilization rate. Assuming no advection ($v_r = v_\theta = v_z = 0$), steady state ($\partial S/\partial t = 0$), no concentration gradient in the z direction, and Monod substrate utilization kinetics, Eq. (12) simplifies to

$$D_S\frac{1}{r}\left(\frac{1}{r}\frac{\partial^2 S}{\partial r^2} + \frac{\partial S}{\partial r}\right) = -\frac{\rho_b}{Y}\frac{\mu_{max}\,S}{K_S + S}. \qquad (13)$$

There is no analytical solution for the above equation, therefore three approximations, numeric, first-order, and zero-order, were generated:

Numeric approximation. The left side of Eq. (13) was numerically integrated by separating the biofilm into radial sections. For the ith biofilm section at axial location n, with a thickness Δr, and $\Delta S = S_{n,i-2} - S_{n,i-1}$:

$$D_S\frac{1}{r}\left(\frac{1}{r}\frac{\Delta^2 S}{\Delta r^2} + \frac{\Delta S}{\Delta r}\right) = -\frac{\rho_b}{Y}\frac{\mu_{max}\,S_{n,i}}{K_s + S_{n,i}}. \qquad (14)$$

Given the left-hand boundary condition and an initial assumption for $\Delta^2S/\Delta r^2$ an iterative solution for the substrate concentration profile through the biofilm can be found.

Flat sheet approximations. Analytical solutions to Eq. (13) may be generated by approximating the biofilm as flat sheet, with a length r_g, the geometric mean radius, and thickness t_b. This approximation will introduce an error, which is expected to be insignificant. Given these assumptions, Eq. (13) simplifies to

$$D_S\frac{\partial^2 S}{\partial r^2} = -\frac{\rho_b}{Y}\frac{\mu_{max}S}{K_S + S}. \qquad (15)$$

In addition, two standard simplifying assumptions are applied in biofilm modeling, as discussed above, to give analytical solutions: (1) zero-order reaction, $S >> K_s$ ($R_S = \rho_b\,\mu_{max}/Y$) and (2) first-order reaction, $S << K_s$ ($R_S = \rho_b\,\mu_{max}S/YK_S$). Given the boundary conditions of Eqs. (8) and (11), the flat sheet, zero-order solution is

$$S = -\frac{\rho_b\,\mu_{max}}{2YD_S}r^2 + \frac{\rho_b\,\mu_{max}t_b}{2YD_S}r + S_{n,m}$$

$$\text{where } t_b = \sqrt{\frac{2YD_S\,(S_{n,i} - S_{n,m})}{\rho_b\mu_{max}}}. \qquad (16)$$

The substrate utilization rate, R_S, can be calculated by integrating over the volume of the biofilm:

$$R_S = 2\pi r_g t_b\,\Delta z\left(\frac{\rho_b\mu_{max}}{Y}\right). \qquad (17)$$

Given the boundary conditions of Eqs. (8) and (11), the flat sheet, first-order solution is

$$S = S_{n,m}e^{-r\sqrt{\frac{\rho_b\,\mu_{max}}{YD_SK_S}}} \text{ where } t_b = -\ln\left(\frac{S_L}{S_{n,m}}\right)\sqrt{\frac{\rho_b\mu_{max}}{YD_SK_S}}. \qquad (18)$$

The substrate utilization rate can be calculated as

$$R_S = 2\pi r_g\Delta z\left(e^{t_b\sqrt{\frac{\rho_b\mu_{max}}{YD_SK_S}}} - 1\right)\sqrt{\frac{\rho_b\mu_{max}}{YD_SK_S}} \qquad (19)$$

Removal in the Reactor

Two spreadsheet programs (MS Excel and QuattroPro versions available) were used to perform the calculations for the three theoretical models. In determining the removal in the biofilm, the numeric model takes an initial assumption of $\Delta^2S/\Delta r^2$ to predict $\Delta S/\Delta r$. The initial $\Delta^2S/\Delta r^2$ approximation is based upon the second derivative of the zero-order approximation of the substrate concentration throughout the biofilm. This assumption is used since the inner face of the biofilm has the highest VOC concentration and therefore the kinetics are closest to zero-order. The zero-order and first-order models estimate the removal in the biofilm in a similar manner. An initial estimate of the biomass thickness is made, from which the substrate concentration at the outer edge of the biofilm is determined. Next the biomass thickness is calculated based on the model prediction of the biomass thickness (t_b). The program preforms an optimization by varying the initial biomass thickness estimate until the difference between the guess and the calculated biomass thickness is negligible. Removal due to the biofilm is then estimated from Eq. (17) or (19).

EXPERIMENTAL METHODS

Batch Culture Studies

Mixed liquor suspended solids (MLSS) were collected from the Amherst, MA, wastewater treatment facility and acclimated to toluene over an eight month period. Cultures were maintained in separate batches that utilized either NO_3^- or

NH_4^+ as a nitrogen source. Twenty-five milliliters of each culture was added to 100 mL of a mineral media solution (MM) in 250-mL glass bottles sealed with Mininert septum caps. Nitrate MM consisted of (g L^{-1}) KH_2PO_4, 3.47; K_2HPO_4, 4.27; $NaNO_3$, 1.59; $MgSO_4 \cdot H_2O$, 0.46; $CaCl_2 \cdot 2H_2O$, 0.018; and $FeSO_4 \cdot 7H_2O$, 0.001, in tap water. In the ammonium MM, the $NaNO_3$ was replaced by 1.23 g/L $(NH_4)_2SO_4$. Toluene was added to an initial headspace concentration of 1000 ppm_v. Bottles were maintained at 27°C with mixing. Approximately every 20 min, a 1.5-mL headspace sample was withdrawn from each bottle and analyzed as discussed below. Volatile suspended solids analysis was performed at the beginning and end of each experiment.

Membrane Materials

Membrane bundles (hollow fiber membranes potted in polysulfone fittings) used in this research were manufactured by Spectrum Microgon (Laguna Hills, CA, P/N CG2M-040-01N). The polypropylene hollow fiber membranes had an inner diameter of 200 μm, an outer diameter of 250 μm, and an active fiber length of 19.5 cm. Porosity (pore density) was nominally 50%, with 0.05 μm nominal pore size. There were 2400 fibers in each bundle and the total outer surface area was 0.37 m^2. The membrane bundle was placed in the "ball" configuration. This configuration allows slack in the fibers so they tend to splay out in a ball shape, allowing for more surface area to be exposed for biofilm formation.

Reactor Configuration

A schematic of the experimental system is shown in Fig. 2. A list of system components is given in Table I. Toluene was continuously added to the inlet airstream using a syringe pump. The rate of air flow was controlled using a gas flow meter.

The bioreactor housing was a 10.5-cm diameter by 28-cm high glass cylinder with anodized aluminum endplates. The overall volume of the system, including recirculation pump and tubing volume, was 3.1 L. An adjustable pressure-regulating valve was used at the liquid outlet to maintain the liquid pressure in the bioreactor at slightly higher than the inlet air pressure. This allowed for bubbleless passage of toluene and oxygen through the membranes.

A nutrient solution containing the microbial culture surrounded the hollow fiber membrane bundle. The nutrient solution was based on the mineral media used in the batch assays, and consisted of (g L^{-1}) KH_2PO_4, 2.43; K_2HPO_4, 2.99; $NaNO_3$, 5.56; $MgSO_4 \cdot H_2O$, 1.61; $CaCl_2 \cdot 2H_2O$, 0.062;

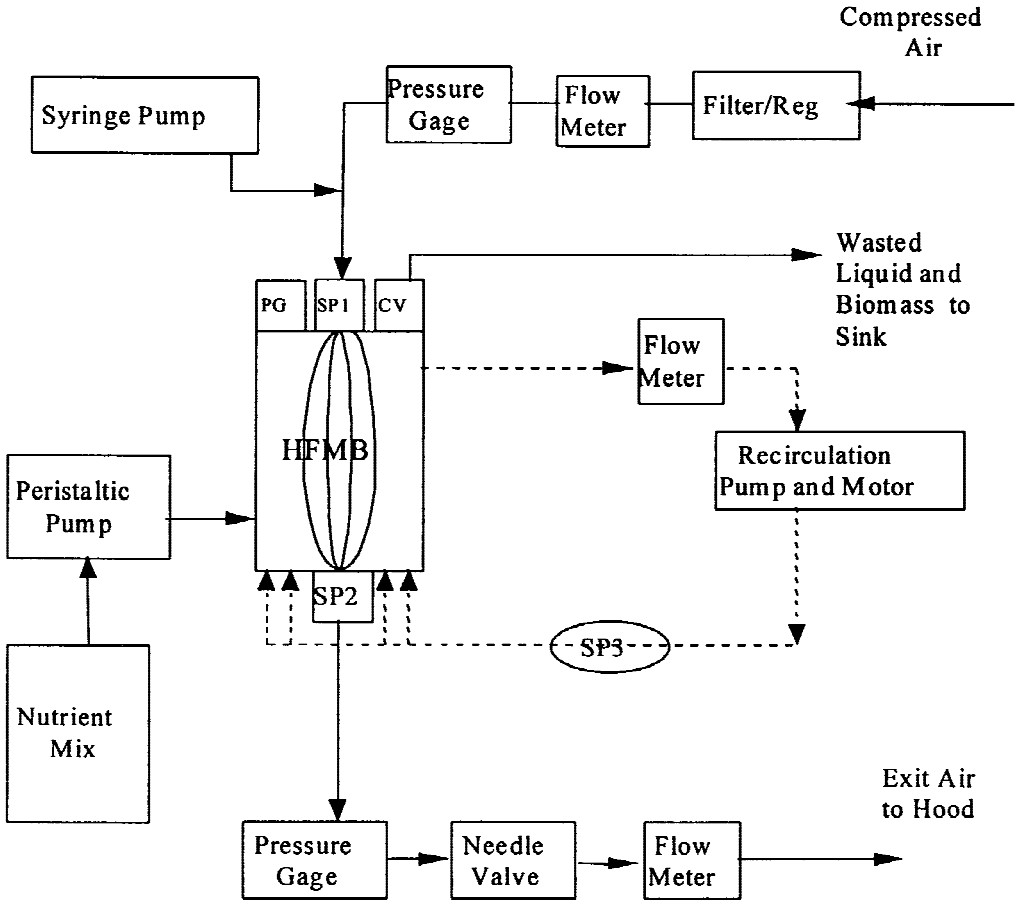

Figure 2. Experimental reactor configuration; SP, sample port; PG, pressure gauge; CV, control valve.

Table I. Experimental system components.

Component	Manufacturer/model
Compressed air filter/regulator	McMaster Carr 500K91
Inlet flow meter	Cole Parmer 63219-21, 0–2.3 L
Inlet pressure gage	Dwyer Instrument Magnehelic 3T323, 0–5 psi
Syringe pump	Harvard Apparatus Model 22
Membrane bundle	Spectrum Microgon CG2M-040-01N
Outlet pressure gage	Dwyer Instrument Magnehelic 3T323, 0–5 psi
Outlet flow meter	Cole Parmer/Gilmont E-03232-22, 0–3.7 L/min
Nutrient media peristaltic pump	Buchler/Labconco 2-6250
CV: pressure regulating valve	Parker 4M-RL4A
PG: liquid pressure gage	Weksler Instruments, 0–30 psi
Liquid flow meter	King Instruments, 0–5 GPM
Recirculation pump/motor	Teel Progressing Cavity 1P610/Dayton 4Z248D

and $FeSO_4 \cdot 7H_2O$, 0.0035, in tap water. A metering pump was used to add MM to the reactor at a flow rate of 8 mL h^{-1}. A variable speed recirculation pump kept the liquid well mixed, and enabled testing of the effect of liquid turbulence on mass transfer.

For the abiotic experiments, the nutrient media feed system was replaced by tubing to a laboratory sink faucet. Water from the sink flowed through the reactor at a rate of either 0.5 or 1.0 L min^{-1} to flush VOCs from the reactor.

Analytical Methods

Gas samples were withdrawn from the inlet and outlet of the reactor through septa using Hamilton gas-tight syringes equipped with SampleLock valves. Gas phase VOC analysis was accomplished using a 30-meter Restek RTX-624 megabore capillary column (isothermally at 100°C with N_2 carrier at 20 mL min^{-1}) in a Varian 3500 GC equipped with a 50-μL sample loop and a flame ionization detector. Detection limits were 2 ppm_v by this method. The GC was calibrated daily using certified hexane standards. Hexane and toluene standards were compared every 2 weeks. All samples were analyzed in duplicate.

Liquid phase toluene concentration was determined using a glass sample bubble inserted in the recirculation loop (Fig. 2). A Mininert septum cap was used to inject air into the top of the bubble. Reactor liquid circulated in the bottom of the bubble. The system was allowed to equilibrate for at least 30 min before sampling and GC analysis of the bubble headspace.

Volatile suspended solids (VSS) analysis was performed using Standard methods 2540 D and E (APHA, 1995). Nitrate concentrations in the bioreactor were measured using Ultraviolet Spectrophotometric Screening, Standard Method 4500 (APHA, 1995). pH of the reactor liquid was determined using a calibrated pH electrode (Orion Model 720A).

Experimental Program

For the abiotic reactor experiments, seven experimental runs were conducted at liquid recirculation rates between 0 and 8.6 L min^{-1}. For each experiment, multiple gas samples were taken at the reactor inlet and outlet to determine steady state toluene removal. For all abiotic experiments, the inlet toluene concentration was 200 ppm_v, the inlet gas flow rate was 1 L min^{-1}, and the inlet gas pressure was 40 cm of water column.

A list of conditions for the bioreactor experiments is given in Table II. The bioreactor was normally sampled every other day throughout the 80-day test. Toluene concentrations were measured in both the gas and liquid phases. Target inlet toluene concentrations varied as much as 25% due to syringe pump fluctuations. This variance had little effect on removal efficiency. For all experiments the inlet gas pressure was 40 cm of water column.

RESULTS

Batch Culture

Batch culture studies were conducted to determine if significantly lower biomass yields could be achieved using nitrate as a nitrogen source rather than ammonium. Previous authors have observed that high biofilm thickness results in decreased membrane bioreactor performance due to diffusion limitations (Freitas dos Santos and Livingston, 1995b; Ergas and McGrath, 1997). Other biofilm control strategies currently under investigation include use of high liquid phase velocities and air scour to shear biomass off the membranes.

Headspace toluene concentrations in all cultures tested decreased from 1000 ppm_v to less than 1 ppm_v over seven hours as shown in Fig. 3. Ammonium cultures acclimated more quickly to toluene than the nitrate cultures. Once the nitrate populations acclimated, however, they degraded toluene at the same rate as the ammonium cultures with a lower biomass yield. Zero-order degradation rate constants and observed biomass yields for all experiments are shown

Table II. Experimental parameters used in bioreactor experiments.

Test	Inlet concentration (ppm_v)	Recirculation rate (L/min)	Inlet flow rate (L/min)
Residence time	200	3.8	0.5
	200	3.8	0.75
	200	3.8	1.0
Substrate loading	200	3.8	0.5
	500	2.8	0.5
	600	2.8	0.5
	1000	2.8	0.5
Liquid velocity	200	0	1.0
	200	1.9	1.0
	200	3.8	1.0
	200	5.7	1.0

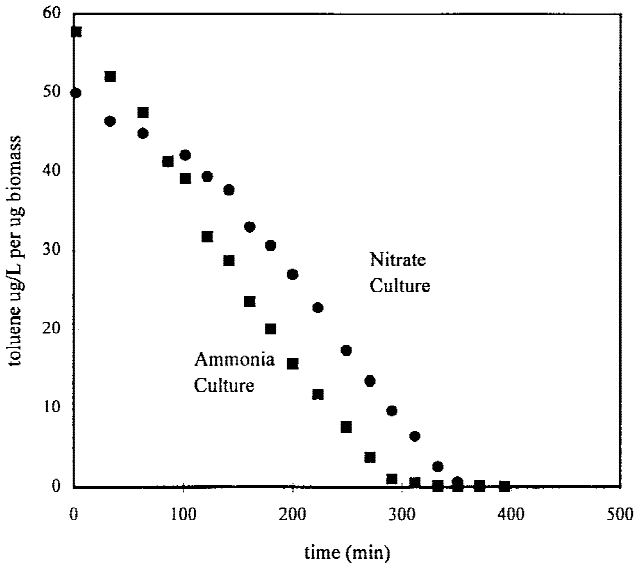

Figure 3. Toluene disappearance in batch cultures utilizing nitrate or ammonia as a nitrogen source.

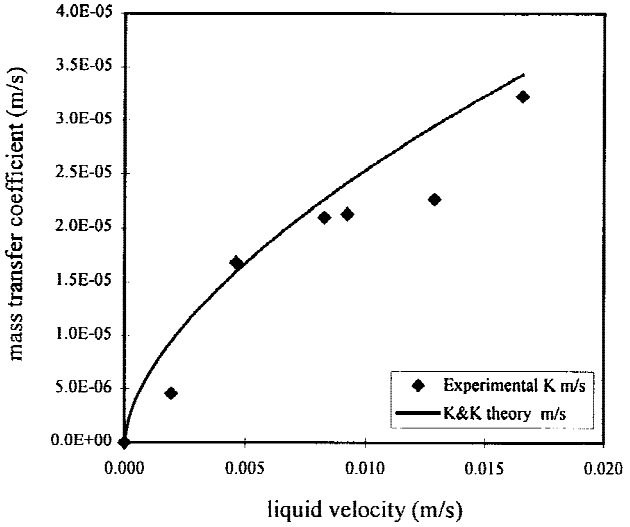

Figure 4. Comparison of mass transfer coefficient determined using Eq. (6) for the experimental system with the Knudsen and Katz correlation (Eq. (4)).

in Table III. These parameters were used in the modeling efforts discussed below.

Abiotic Mass Transfer

Experiments were performed to determine baseline performance of the system in the absence of a biofilm and to determine the effect of liquid recirculation on mass transfer rate. Mass transfer coefficients (determined from experimental data using Eq. (6)) increased with increasing liquid phase velocity, as shown in Fig. 4. The Knudsen and Katz heat transfer coefficient correlation (Eq. (4)) gave a reasonable estimate of the mass transfer coefficients for the system. A comparison of the data with the Knudsen and Katz model is also shown in Fig. 4.

Bioreactor Acclimation

A plot of toluene removal efficiency vs time during the first 18 days after inoculation of the reactor with the nitrate-utilizing cultures is shown in Fig. 5. Inlet toluene concentration was 200 ppm_v and gas residence time was 1.8 s during this period. Initially, inlet and outlet toluene concentrations were equal, indicating that physical/chemical removal processes were not significant in this system. On the day after reactor inoculation with the pre-acclimated suspended culture, a sharp increase in toluene removal was observed. On the third day, the reactor liquid was clear, biofilm attachment to the membranes was observed, and toluene removal efficiency decreased by 50%. Over the next seven days, removal efficiency gradually increased as the biofilm grew denser.

Arcangeli and Arvin (1992) and Reij et al. (1992) also observed this phenomenon in fixed-film bioreactors degrading toluene and propene respectively. The authors attributed the drop in removal efficiency to starvation conditions in the liquid phase. As the biofilm attached to the membranes and the density increased, higher removal efficiencies were observed.

An alternate explanation for the drop in removal is increased mass transfer resistance due to changes in the hy-

Table III. Growth phase toluene degradation rates and observed yield.

Sample	Degradation rate (μg toluene/μg biomass/day)	Observed yield (μg biomass/μg toluene)
Culture A–ammonia	42	0.41
Culture A–nitrate	42	0.24
Culture B–ammonia	33	0.61
Culture B–nitrate	33	0.45

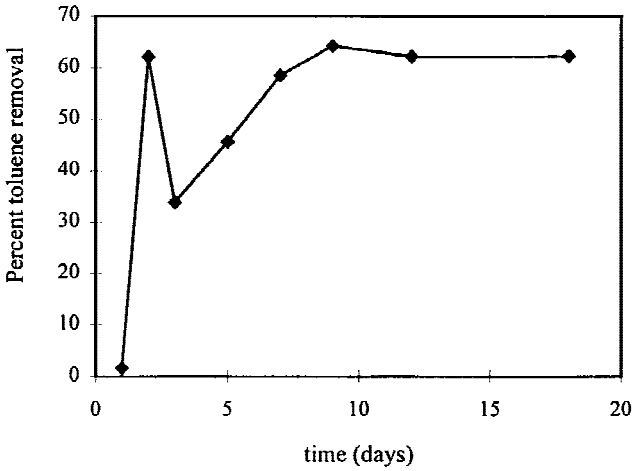

Figure 5. Toluene removal efficiency during the acclimation phase of the bioreactor studies.

drophobicity of the membranes. Toluene from the gas phase and polysaccharide materials from the biomass could coat the pore surfaces of the membrane, decreasing hydrophobicity and causing water to fill some pores. This would result in increased membrane phase resistance ($1/k_m$). Lund (1996) observed this phenomenon in blood oxygenation systems, with increases in mass transfer resistance of several orders of magnitude. Lipids were found to act as surfactants that changed the hydrophobicity of the membranes.

Toluene removal efficiency reached steady state 9 days after inoculation. Thereafter, the biofilm appeared to have uniform density along the fibers but was denser on fibers towards the center of the membrane bundle where there was more protection from liquid phase turbulence.

Steady State Bioreactor Performance

A summary of the steady state bioreactor performance data is shown in Table IV. Three sets of experiments were performed: (1) gas residence was varied by changing the gas flow rate and maintaining the inlet concentration at 200 ppm_v, (2) toluene loading rate was varied by changing the inlet toluene concentration while maintaining the gas flow rate at 0.5 L/min, and (3) liquid recirculation flow rate was varied from 0 to 5.7 L min^{-1}.

Toluene elimination capacity increased with increasing gas residence time and substrate loading rate, however, elimination capacity appeared to reach a maximum of 42 g m^{-3} min^{-1}. Although mass transfer rate was highly dependent on liquid phase velocity in the abiotic system, no effect was observed on toluene removal efficiency at any flow rate once the biofilm was established. Liquid phase turbulence does not appear to affect mass transfer rate, except indirectly by controlling biofilm thickness.

Biofilm Models

Model simulations were performed using the three biofilm models and the parameters shown in Table V. Experimental conditions and results, given in Tables II and IV respectively, were used to determine if the models could predict observed removals. None of the models initially accurately predicted VOC removal efficiency. To fit the models, the biofilm density was varied until the predicted removal matched the observed removal. All three models were fit to a single experimental observation (1.8-s gas residence time, 3.8 L min^{-1} liquid flow rate). The zero- and first-order models predicted removal poorly, as shown in Fig. 6. In addition, values of ρ_b fit to the first- and zero-order models were 40 and 0.4 mg L^{-1}, respectively, several orders of magnitude lower than the literature values (Characklis and Marshall, 1990). Poor prediction of removal with these models is not surprising because the concentration in the biofilm varies from well above to well below the half saturation value, spanning both zero- and first-order behavior. Due to the poor performance of these models, no further analysis was performed with them.

The numeric model fit the observed removal fairly well, as shown in Fig. 6. The biofilm biomass density was calibrated at 29,000 mg L^{-1}, slightly higher than that reported by Characklis and Marshall (1990). The numeric model predicted the observed trend that the liquid turbulence, or flow rate, had little effect on observed removal. The numeric model slightly underpredicted the effect that substrate loading had on removal in the system.

The only case of poor prediction by the numeric model was the effect of gas residence time on removal. Observed removals were higher than predicted removals for these runs. If the pore space of the membranes became water-filled during the course of experimentation, as discussed above, an added resistance to mass transfer would be expected, and mass transfer to the biofilm could become dependent upon the gas flow rate (gas-to-liquid transfer).

The numeric model was modified to account for the possibility of mass transfer resistance through the water-filled pores of the membrane (Eq. (7)). The concentration at the biofilm inner surface, $S_{n,0}$, was approximated by the concentration predicted for a stagnant liquid film. If a stagnant liquid film with no biological activity stretched between the

Table IV. Summary bioreactor performance over the four month experimental program.

Test	Gas residence time (s)	Liquid flow rate (L/min)	Inlet conc. (ppm)	Toluene loading rate ($g/m^3/min$)	Removal efficiency (%)	Elimination capacity ($g/m^3/min$)
Residence time	0.9	3.8	194	52	55	28
	1.2	3.8	201	45	68	30
	1.8	3.8	193	26	71	18
Substrate loading	1.8	2.8	220	29	72	21
	1.8	2.8	499	66	54	36
	1.8	2.8	620	82	43	35
	1.8	2.8	914	121	35	42
Liquid velocity	1.8	0	200	27	70	18
	1.8	1.9	174	23	68	16
	1.8	2.8	220	29	72	21
	1.8	3.8	193	26	71	18
	1.8	5.7	185	25	72	18

Table V. Parameter estimates for the biofilm models.

Parameter	Value	Source
Outer diameter, d_{out}	0.25 mm	Manufacturer
Inner diameter, d	0.20 mm	Manufacturer
Number of fibers, n	2400	Manufacturer
Fiber length, L	19.5 cm	Manufacturer
Fiber division, Δz	5 mm	Assumed
Henry's law coefficient, H	0.27	Montgomery and Welkom, 1989
First order rate constant, k	33 day^{-1}	Measured
Yield coefficient, Y	0.24 mg mg^{-1}	Measured
Half saturation constant, Ks	0.02 mg/L	Corseuil and Webber, 1994
Liquid mass transfer coeff., k_1	varied	Eq. (4)
Liquid diffusion coeff., D_L	8.5×10^{-10} m^2s^{-1}	Reid et al., 1977
Biofilm diffusion coeff., D_S	$0.8*D_L$	Rittmann and McCarty, 1980
Biofilm biomass density, ρ_b	25,000 mg L^{-1}	Characklis and Marshall, 1990
Liquid biomass density, ρ_L	1 mg L^{-1}	Measured
Total reactor volume, V	2.4 L	Measured

gas/liquid interface and the bulk fluid, the concentration at any point can be determined as (Bird et al., 1960):

$$\left(\frac{S_{n,0}}{HC_n}\right) = \left(\frac{S_L}{HC_n}\right)^{\frac{r-r_i}{r_o-r_i}}, \quad (20)$$

where r_i is the inner radius of the membrane and r_o is the outer radius of the membrane with 0.1 mm added (biofilm thickness approximation). The resulting toluene concentration at the inner biofilm decreased to roughly one-eighth the prior value, and removal decreased correspondingly. When the biofilm thickness was increased to 35,000 mg/L to fit the experimental datum, the predicted removals for the other experiments were all low, as reflected in Figure 6. Further experimentation is required to clarify the difference between model predictions and observed removal.

Sensitivity Analysis

A sensitivity analysis was conducted on the numeric model to determine (1) if the assumptions had a large effect on predicted removal and (2) the apparent effect of varying operational parameters on system performance. The yield, liquid mass transfer coefficient, and liquid substrate concentration had little effect on predicted removal in the system. The liquid phase biomass density, however, had a significant effect when it was greater than 10 mg L^{-1}. This was expected since a higher biomass density significantly increases liquid phase removal. Similarly, the suspension volume attributed to the *n*th section of a single lumen has a significant effect when it becomes greater than 0.1 mL. The half saturation constant has a significant impact, decreasing the removal rate when it approaches the substrate concentration at the inner edge of the biofilm. The effect of the biomass density on predicted removal is shown in Fig. 7. The relationship appears to be linear for values below 10,000 mg/L and then approaches a maximum of approximately 80%. The effect of μ_{max} was similar to the effect of biofilm density, as expected (μ_{max} and ρ_b are essentially a single parameter in Monod kinetics). The relationship of the biofilm diffusion coefficient and predicted removal is also

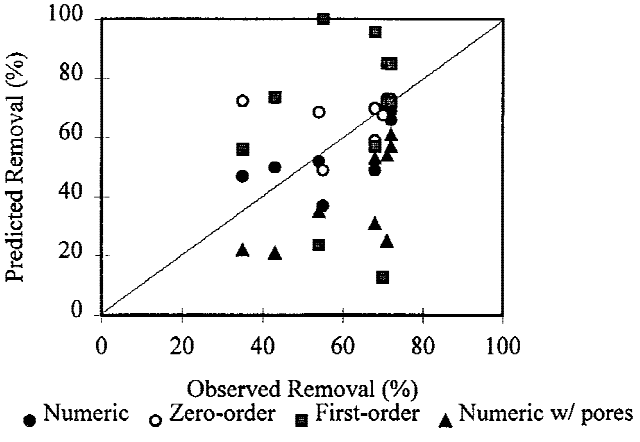

Figure 6. Comparison of predicted and observed percent removals.

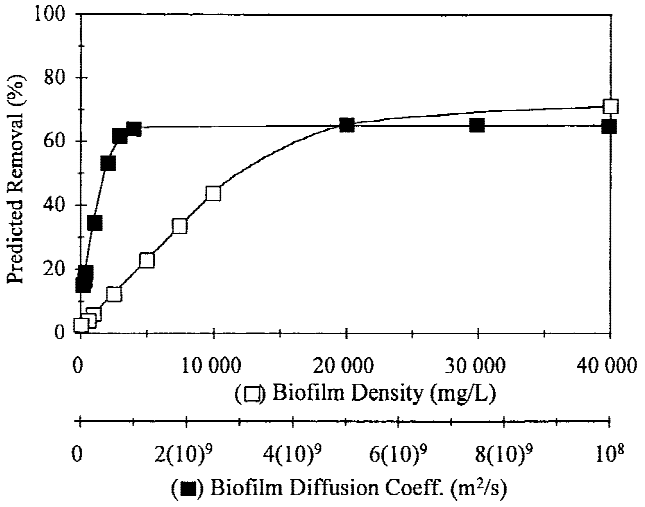

Figure 7. Sensitivity of removal as a function of biofilm density and biofilm diffusion coefficient.

shown in Fig. 7. Small changes in the estimate of D_S (approximately 7×10^{-10} m^2 s^{-1}) have a significant effect on predicted removal of the system. The current biofilm diffusion coefficient was based upon the assumption that the biofilm diffusion coefficient is approximately 80% of the liquid diffusion coefficient (Rittmann and McCarty, 1980). Other investigators have found that the relationship can be as little as 17% of the liquid diffusion coefficient (Beyenal et al., 1997). This suggests that selection of a biofilm diffusion coefficient is critical to the model prediction and that increased removals can be achieved for compounds with higher diffusion coefficients.

CONCLUSIONS

This study demonstrated sustained removal of 200 ppm_v toluene from an air stream using a membrane biofilter. Removals ranged from 28% to 72%, with removal efficiency directly related to gas residence time and inversely related to the substrate loading. Although liquid turbulence dominated mass transfer in the abiotic case, with the Knudsen–Katz correlation predicting mass transfer, the removal in the bioreactor was not affected by the liquid flow rates examined. The maximum elimination capacity for the conditions studied was 42 g m^{-3} min^{-1}.

The bioreactor seed, isolated from the Amherst WWTP, exhibited similar degradation kinetics whether grown on ammonium-N or nitrate-N, but the yield on nitrate was one-half to two-thirds of that on ammonium. When the bioreactor was seeded, initial removal was high, subsided, and then returned to high levels, possibly due to mass transfer affects associated with biofilm formation. Nine days were required after seeding to achieve stable removal.

Three models of the reactor were created: a numeric model, a first-order flat sheet model, and a zero-order flat sheet model. Only the numeric model fit the data well, although removal predicted as a function of gas residence time disagreed slightly with that observed. A modification in the numeric model to account for membrane phase resistance resulted in an underprediction of removal. Sensitivity experiments with the numeric model indicated that removal was a strong function of the biofilm phase biomass density and also of the biofilm diffusion coefficient, with diffusion rates below 10^{-9} m^2 s^{-1} resulting in decreased removal rates. This membrane biofilter system shows great promise as a treatment system for high gas loading rates and chlorinated organic compounds that currently cannot be treated using conventional biofilters.

Nomenclature

a	membrane surface area per unit volume (1/L)
A	membrane surface area (L^2)
A_b	biofilm outer surface area (L^2)
A_m	membrane surface area in a section (L^2)
C_g	gas phase concentration (mass/L^3)
C_n	gas phase concentration in the nth section (mass/L^3)
$C_{n,m}$	gas phase concentration on the outer face of the membrane (mass/L^3)
C_o	inlet gas phase concentration (mass/L^3)
d	membrane diameter (L)
d_e	effective diameter for calculating Re (L)
D_s	diffusion coefficient in the biofilm (L^2/time)
H	Henry's law coefficient (dimensionless)
J	mass flux from the gas phase to the liquid phase (mass/time)
J_b	mass flux from biofilm to liquid suspension (mass/time)
J_n	mass flux through the membrane in the nth section (mass/time)
K	overall mass transfer coefficient (L/time)
k_g, k_L, k_m	gas, liquid and membrane mass transfer coefficients (L/time)
K_S	Monod half-saturation coefficient (mass/L^3)
Q	liquid flow rate in the suspension (L^3/time)
Re	Reynolds number (dimensionless)
r_i,r_o	inner and outer radius of the membrane (L)
r_g	geometric mean radius (L)
R_s	substrate utilization rate (mass/L^3-time)
S	biofilm phase concentration (mass/L^3)
Sc	Schmitt number (dimensionless)
Sh	Sherwood number (dimensionless)
S_L	liquid phase concentration in the suspension (mass/L^3)
$S_{n,0}$	concentration at the membrane biofilm interface in the nth section (mass/L^3)
$S_{n,i}$	concentration at the outer edge of the biofilm in the nth section (mass/L^3)
S_O	concentration entering the suspension (mass/L^3)
t_b	biofilm thickness (L)
V	suspension volume (L^3)
v_r, v_θ, v_z	velocity in the r, θ, or z direction (L/time)
v_L	velocity in the suspension (L/time)
Y	yield coefficient (mass/mass)
ν	kinematic viscosity (L^2/time)
Δ_r	thickness of biofilm section (L)
Δ_z	vertical length of nth section (L)
μ_{max}	Monod maximal specific growth rate (1/time)
ρ_b	biomass density in the biofilm (mass/L^3)
ρ_L	biomass density in the suspension (mass/L^3)

This material is based on work supported by the National Science Foundation under Grant No. BES-9530592. Any opinions, findings, conclusions, or recommendations expressed in this material are those of the authors and do not necessarily reflect the views of the National Science Foundation. Ms. Shumway was supported by the Department of Defense Environmental Fellowship Program. The biofilm modeling is part of the work supported by an Oak Ridge Associated Universities Junior Faculty Enhancement Award to M.W.F.

References

Ahmed T, Semmens MJ. 1992. Use of sealed end hollow fibers for bubbleless membrane aeration: experimental studies. J Membr Sci 69:11–20.

Ahmed T, Semmens MJ. 1996. Use of transverse flow hollow fibers for bubbleless membrane aeration. Water Res 30:440–446.

American Public Health Association. 1995. Standard methods for the examination of water and wastewater. 19th ed. Washington, DC: APHA.

Arcangeli JP, Arvin E. 1992. Toluene biodegradation and biofilm growth in an aerobic fixed-film reactor. Appl Microbiol Biotechnol 37: 510–517.

Aziz CE, Fitch MW, Linquist LK, Pressman JG, Georgiou G, Speitel GE Jr. 1995. Methanotrophic biodegradation of trichloroethylene in a hollow fiber membrane bioreactor. Environ Sci Technol 29:2574–2583.

Beyenal H, Seker S, Tanyolac A, Salih B. 1997. A mathematical model for hollow fiber biofilm reactors. AIChE J 43:243–250.

Bird RB, Stewart WE, Lightfoot EN. 1960. Transport Phenomena. New York: Wiley.

Castro K, Zander AK. 1995. Membrane air stripping: Effects of pretreatment. J Am Water Works Assoc 87:50–61.

Characklis WG, Marshall KC. 1990. Biofilms. New York: Wiley.

Corseuil HX, Weber WJ Jr. 1994. Potential biomass limitations on rates of degradation of monoaromatic HCs by indigenous microbes in subsurface soils. Water Res 28:1415–1423.

Coté P, Bersillon JL, Huyard A, Faup G. 1988. Bubble-free aeration using membranes: process analysis. J Water Pollution Control Fed 60: 1986–1992.

Coté P, Bersillion JL, Huyard A. 1989. Bubble-free aeration using membranes: Mass transfer analysis. J Membr Sci 47:91–106.

Cunningham AB, Visser E, Lewandowski Z, Abrahamson M. 1995. Evaluation of a coupled mass transport–biofilm process model using dissolved oxygen microsensors. Water Sci Technol 32:107–114.

Ergas SJ, McGrath MS. 1997. Membrane bioreactor for control of volatile organic compound emissions. J Environ Eng ASCE 123:593–598.

Freitas dos Santos LM, Livingston AG. 1995a. Membrane-attached biofilms for VOC wastewater treatment I: novel in situ biofilm thickness measurement technique. Biotechnol Bioeng 47:82–89.

Freitas dos Santos LM, Livingston AG. 1995b. Membrane-attached biofilms for VOC wastewater treatment II: effect of biofilm thickness on performance. Biotechnol Bioeng 47:90–95.

Hartmans S, Leenen EJTM, Voskuilen GTH. 1992. Membrane bioreactor with porous hydrophobic membranes for waste-gas treatment. In: Dragt AJ, van Ham J, eds. Biotechniques for air pollution abatement and odour control policies. Amsterdam: Elsevier Science Publishers.

Kim BR, Suidan MT. 1989. Approximate algebraic solution for a biofilm model with the Monod kinetic expression. Water Res 23:1491–1498.

Knudsen JG, Katz DL. 1958. Fluid dynamics and heat transfer. New York: McGraw-Hill.

Lund LW, Federspiel WJ, Walters FR, Hattler BG. 1996. A novel method for measuring hollow fiber membrane permeability in gas–liquid system. ASAIO J 42:M446–M451.

Mirpuri R, Sharp W, Villaverde S, Jones W, Lewandowski Z, Cunningham A. 1997. Predictive model for toluene degradation and microbial phenotypic profiles in flat plate vapor phase bioreactor. J Environ Eng 123:586–592.

Montgomery JH, Welkom LM. 1989. Groundwater chemicals desk reference. Chelsea, MI: Lewis.

Parvatiyar MG, Govind R, Bishop DF. 1996a. Biodegradation of toluene in a membrane biofilter. J Membr Sci 119:17–24.

Parvatiyar MG, Govind R, Bishop DF. 1996b. Treatment of trichloroethylene (TCE) in a membrane biofilter. Biotechol Bioeng 50:57–64.

Pavasant P, Freitas dos Santos LM, Pistikopoulos EN, Livingston AG. 1996. Prediction of optimal biofilm thickness for membrane-attached biofilms growing in an extractive membrane bioreactor. Biotechnol Bioeng 52:373–386.

Reid RC, Prausnitz JM, Sherwood TK. 1977. The properties of gases and liquids. New York: McGraw-Hill.

Reij MW, de Gooijer KD, de Bont JAM, Hartmans S. 1995. Membrane bioreactor with a porous hydrophobic membrane as a gas-liquid contactor for waste gas treatment. Biotechnol Bioeng 45:107–115.

Reij MW, Hamann EK, Hartmans S. 1997. Biofiltration of air containing low concentrations of propene using a membrane bioreactor. Biotechnol Prog 13:380–386.

Rittmann BE, McCarty PL. 1980. Model of steady state biofilm kinetics. Biotechnol Bioeng 22:2343–2357.

Saez PB, Rittmann BE. 1988. Improved pseudoanalytical solution for steady-state biofilm kinetics. Biotechnol Bioeng 32:379–385.

Saez PB, Rittmann BE. 1990. Error analysis of limiting-case solutions to the steady-state biofilm model. Water Res 24:1181–1185.

Semmens MJ, Quen R, Zander AK. 1989. Using a microporous hollow-fiber membrane to separate VOCs from water. J Am Water Works Assoc 81:162–167.

Shen Z, Huang J, Qian G. 1997. Recovery of cyanide from wastewater using gas-filled membrane absorption. Water Environ Res 69: 363–367.

Villaverde S, Mirpuri R, Lewandowski Z, Jones WL. 1997. Study of toluene degradation kinetics in a flat plate vapor phase bioreactor using oxygen microsensors. Water Sci Technol 36:77–84.

Wanner O. 1995. New experimental findings and biofilm modeling concepts. Water Sci Technol 32:133–140.

Yang MC, Cussler EL. 1986. Designing hollow-fiber contactors. AIChE J 32:1910–1916.